BELLCOMM, INC.
1100 SEVENTEENTH STREET, N.W.   WASHINGTON, D.C.   20036

COVER SHEET FOR TECHNICAL MEMORANDUM

TITLE- A Monte Carlo Analysis of SCS
ΔV Mode Powered Flights on
the Transearth Leg of an
Apollo Lunar Mission

FILING CASE NO(S)- 310

FILING SUBJECT(S)- Abort Guidance
(ASSIGNED BY AUTHOR(S)- Error Analysis
Transearth Injection
Entry Errors

TM-67-2012-5

DATE- September 11, 1967

AUTHOR(S)- D. A. Corey

ABSTRACT

A Monte Carlo dispersion analysis of the performance
of the Apollo Spacecraft backup guidance system on the Trans-
earth leg of a lunar mission has been conducted. The primary
purpose was to determine whether the errors at Entry were small
enough so that a spacecraft with a low lift-to-drag ratio could
successfully effect Entry.

The flight path angle and azimuth errors at Entry were
found to be adequately small provided MSFN navigation is used.

X68-81179
(ACCESSION NUMBER)   (THRU)

(PAGES)   (CODE)

(NASA CR OR TMX OR AD NUMBER)   (CATEGORY)

FF No. 602(B)

SEE REVERSE SIDE FOR DISTRIBUTION LIST

DISTRIBUTION

<u>COMPLETE MEMORANDUM TO</u>

CORRESPONDENCE FILES:

OFFICIAL FILE COPY
plus one white copy for each
additional case referenced

TECHNICAL LIBRARY (4)

<u>OMSF</u>

T. A. Keegan - MA ←——COPY TO

<u>MSC</u>

R. L. Berry - FM5
D. C. Cheatham - EG
A. Cohen - PD
K. J. Cox - EG23
T. F. Gibson, Jr. - FS5
H. W. Tindall, Jr. - FM
R. J. Ward - PM
J. D. Yencharis - FM5

<u>BELLCOMM</u>

D. R. Anselmo
A. P. Boysen, Jr.
J. O. Cappellari, Jr.
D. R. Hagner
W. G. Heffron
W. C. Hittinger
B. T. Howard
M. G. Kelly
H. S. London
J. L. Marshall, Jr.
J. Z. Menard
V. S. Mummert
I. D. Nehama
B. G. Niedfeldt
D. J. Roek
I. M. Ross
R. V. Sperry
R. L. Wagner
D. P. Woodard
Department 1023

<u>COVER SHEET ONLY TO</u>

BA-146 (8-64)

SUBJECT: A Monte Carlo Analysis of SCS
ΔV Mode Powered Flights on
the Transearth Leg of an
Apollo Lunar Mission
Case 310

DATE: September 11, 1967

FROM: D. A. Corey

TM-67-2012-5

TECHNICAL MEMORANDUM

1.0 INTRODUCTION

There has been considerable concern recently, that
the current estimates of the Apollo command module lift-to-
drag ratio places a constraint on the tolerable Entry corri-
dor which cannot be achieved under some worst case conditions.
One of these worst cases is where the Command Module must per-
form the Transearth Injection (TEI) maneuver and subsequent
midcourse corrections using its backup guidance system. This
memorandum reports the results of a study to evaluate the
expected dispersions at Entry under this condition.

The backup guidance system utilizes the three body-
mounted gyros in the Stabilization Control System (SCS) as
an attitude reference and a single accelerometer to measure
the change in velocity (ΔV). In preparation for an SCS ΔV
mode maneuver the RTCC computes the desired inertial attitude,
the time of ignition, and the ΔV required for the maneuver
and sends these to the spacecraft. The astronauts align the
spacecraft to the desired inertial attitude and initiate the
maneuver. A display indicates the measured ΔV to the astro-
nauts and the engine is shutdown when the desired ΔV is
achieved. During the maneuver, the SCS maintains the desired
inertial attitude. The performance of the entire system is
considerably poorer than the performance of the primary guid-
ance system for three reasons. First, the individual system
components are not as accurate as the components in the prime
system. In addition, the astronauts cannot align the vehicle
as accurately if the sextant is inoperable. Secondly, with
only a single accelerometer, no facility exists for directly
measuring acceleration in the directions orthogonal to the
accelerometer input axis. Thirdly, the ΔV mode does not adapt
to sensed deviations since no facility exists for computing
or commanding a new attitude and desired ΔV during the maneu-
ver. For these reasons, the backup scheme provides substan-
tially degraded performance when compared to the primary
system, and therefore could require greater allowable disper-
sions at Entry.

2.0 METHODS AND ASSUMPTIONS

The statistics of the Entry dispersions were formed from 551 Monte Carlo simulations of the entire Transearth leg of the mission. Each of the runs was simulated as follows: Random samples were taken from each of the error source distributions in preparation for the simulation of the TEI maneuver. The actual state vector and the guidance estimate of the state vector were integrated through the burn using the actual and estimated thrust acceleration vectors respectively. The nominal (no error) final state vector was then subtracted from the final actual and estimated state vectors for the error cases, forming the actual and estimated state vector dispersions at the end of TEI. These dispersions were next propagated with free fall transition matrices out to the time of the first scheduled midcourse correction. The estimated state vector deviations were set equal to the actuals at this point, simulating a perfect state vector update prior to the correction. The required midcourse correction was then calculated and performed for each of the 551 samples. The resulting state vector dispersions were then propagated on to the time of the second midcourse correction. A second correction was performed, the results propagated to the time of the third midcourse correction, and the third correction was made. The actual dispersions at the end of the third correction were propagated forward to the nominal Entry altitude.

A perfect state vector update was assumed prior to each of the midcourse corrections and prior to TEI. It was felt that the uncertainties in the state vector due to nonperfect MSFN tracking were negligible in comparison to the execution errors in the maneuvers. A previous study (Reference 1) has shown this to be true for the primary guidance system in the TEI maneuver.

The midcourse corrections simulated were finite time powered flight maneuvers with basically the same set of error sources as the TEI maneuver.

It should be stressed that complete powered flight simulations were made for each powered flight phase so that any nonlinear effects were included. The Monte Carlo approach was used because of the difficulties involved in generating linear transition matrices for the midcourse correction maneuvers.

2.1 Free Flight Propagation

Propagation of the dispersions through the free fall portions of the mission was accomplished using linear transition matrices except for the portion between the third midcourse

and Entry. The transition matrices were generated by inte-
grating deviations from the reference trajectory between the
points of interest. The validity of the linearity assumption
was tested by selecting several samples obtained at various
points in the simulation and integrating them forward to the
point of interest. The integrated results were then compared
with the results from the linear transition matrix propagation.
Excellent agreement was obtained. The state vectors at the
end of the third midcourse correction were individually propa-
gated forward to the reference trajectory Entry altitude.
This propagation was performed using two-body conic equations.
The dispersions about the propagated nominal state vector were
computed and used as the dispersions about the reference tra-
jectory Entry state vector.

2.2 Midcourse Correction Models

Each of the three midcourse corrections were made at
a specified time. The first correction occurred 19 hours after
TEI. The second occurred 15 hours prior to Entry. The third
occurred 5 hours prior to Entry.

The required corrections were computed on the basis
of achieving the reference Entry position at the reference
time. This was accomplished in the following manner.

Let $[\phi_{21}]$ be the linear transition matrix which re-
lates deviations at the midcourse time to deviations at the
time of reference Entry. $[\phi_{21}]$ is a six-by-six matrix which
is partioned into four three-by-three matrices.

$$[\phi_{21}] = \left[\begin{array}{c|c} M_{21} & N_{21} \\ \hline S_{21} & T_{21} \end{array} \right]$$

If $\vec{\delta X}_{mc}$ is the state vector deviation at the midcourse time,
then the position miss at Entry is given by

$$\vec{\delta P}_E = [M_{21} | N_{21}] \; \vec{\delta X}_{mc}$$

The velocity correction at the midcourse time necessary to drive $\vec{\delta P}_E$ to zero is given by

$$\vec{\Delta V}_{mc} = -[N_{21}{}^{-1}] \; [M_{21} \; N_{21}] \; \vec{\delta X}_{mc}$$

Again, the linearity assumptions were verified by selecting several sets of deviations at each of the midcourse points and determining the midcourse required by a targeting procedure using integrated trajectories. The velocity corrections thus obtained were compared with the corrections computed using the linear transition matrices and excellent agreement was obtained.

The criteria for determing whether or not to make a correction varied with the midcourse. For the first two corrections, no correction was made if ΔV_{req}, the magnitude of the required velocity change, was less than one fps or if $5 < \Delta V_{req} < 17$. If $1 \leq \Delta V_{req} \leq 5$, the correction was made using the RCS thrusters only. If $\Delta V_{req} > 17$, a five fps ullage with the RCS thrusters was made and the remainder of ΔV_{req} was obtained with the main (SPS) engine.

For the third midcourse, no correction was made if $\Delta V_{req} < 1$ fps. If $1 \leq \Delta V_{req} < 17$, the correction was made using the RCS thrusters. If $\Delta V_{req} \geq 17$, a five fps ullage was made with the RCS thrusters and the remainder was obtained with the SPS engine.

2.3 Powered Flight Error Models

Table 1 presents the values of the error sources assumed for this study. Locating documented values for several of the error sources proved to be one of the more difficult tasks in the study. As a consequence, some values were selected on the basis of seeming reasonable and no documented source is offered. Unfortunately, one of these turned out to be a principal error source. That was initial misalignment of the body about the body pitch axis. This error source reflects how well the astronaut can align the spacecraft to a desired inertial attitude and how accurately the body mounted gyros can control

the rotation of the vehicle to the desired attitude for the maneuver. Since this was a "worst case" study, the sextant was assumed inoperative and the astronaut would have to align the body by looking at stars or landmarks through the window. The assumed initial misalignment error of 0.5 degrees one sigma about all three axis seemed reasonable. Related to this problem is the amount of time between the time the astronaut aligns the body and uncages the gyros, and the time of engine ignition. This can be important since it involves the amount of time the gyros drift before ignition. The value assumed was 30 minutes.

No data could be found for specific accelerometer errors such as bias or scale factor. These effects are, however, included in the total ΔV counter error.

Because not all error sources behave the same, two types of error sampling was used. For some error sources, the same error value was used for all maneuvers. For example, if the SPS thrust in TEI was four pounds greater than nominal, it was also four pounds greater for the associated midcourse corrections. For other error sources, different random values were selected for each maneuver. An example of the latter is the initial misorientation of the body thrust axis. Table 1 indicates whether the same random values were used for all maneuvers on a flight or if different values were selected for each maneuver.

A random value for the vehicle mass uncertainty was selected only at the beginning of TEI. The mass at the end of TEI for each monte carlo run was used as the initial mass at midcourse 1, etc.

While no autopilot or engine control system was modeled, the reaction of the vehicle to a center of gravity uncertainty was modeled. Figure 1 presents the vehicle attitude error as a function of time since ignition in response to the one sigma c.g. uncertainty of 0.5 degrees (Reference 5). This figure is valid for both the pitch and yaw directions. This error was considered for the SPS portion of the maneuvers only.

2.4   Reference Trajectory

The reference trajectory selected for study was the 504 Preliminary Reference Trajectory (Reference 2). Table 2 presents some of the trajectory parameters of interest as well as nominal vehicle performance parameters assumed for the study.

Since the reference trajectory TEI maneuver was guided according to the cross product steering law, the TEI maneuver had to be retargeted slightly for this study. The retargeting was done to enable the TEI maneuver to be performed with a constant inertial attitude so as to arrive at Entry at the reference trajectory time and with the reference flight path angle. All other Entry parameters of the retargeted trajectory agreed very well with the reference trajectory.

TEI ignition occurred at reference time. The nominal inertial attitude was that which would be obtained from the initial commanded attitude of the cross product steering law with the guidance constant equal to 0.466055. The required TEI ΔV was 2654.8251 fps.

3.0 DISCUSSION OF RESULTS

Table 3 presents the sample covariance matrix obtained at the end of TEI. The matrix is in the orbit plane or UVW coordinate system in which U is along the nominal position vector, W is in the direction of the nominal angular momentum vector, and V completes the right handed orthogonal system.

This covariance matrix was compared with the covariance matrix of actual dispersions obtained using the primary guidance system (see Reference 3). The velocity errors at the end of TEI for the SCS ΔV mode are on the order of 15 times larger - indicating considerably degraded performance.

The large $\dot{U}$, or radial velocity errors, were principally caused by two error sources, initial misalignment about the pitch axis, and pitch gyro constant drift. The large $\dot{V}$ or downrange velocity errors were caused principally by the ΔV counter error.

The above mentioned three error sources together with initial misalignment about the yaw axis and yaw gyro constant drift were the only error sources which contributed materially to the dispersions at the end of TEI. The latter two error sources caused the substantial out of plane velocity errors.

Table 4 presents the sample covariance matrix of the actual dispersions at Entry. This covariance matrix was compared with several of the Entry covariance matrices generated in the study described by Reference 1. The SCS ΔV mode Entry errors are considerably larger (by two orders of magnitude) than the errors obtained using the primary guidance system and MSFN navigation. They were also very slightly larger than

the errors obtained using the primary guidance system with
the on-board optical navigation system. They were however,
considerably smaller than the errors obtained when the sex-
tant accuracy was assumed to be three times worse than its
specification value.

The primary reason that the SCS ΔV mode errors were
slightly smaller is that the third midcourse corrections were
generally quite small. In fact in about 55% of the cases they
were either not made at all or only the RCS system was required.
This avoided the rather large pointing errors associated with
a short SPS burn due to the center of gravity location uncer-
tainty. In addition, the ΔV counter errors are much smaller
for small ΔV maneuvers. In the case of the on-board navigation
system however, the third midcourse correction was subject to
considerable error because of large landmark uncertainties even
though the midcourse execution was better than in the SCS ΔV
mode case.

Since the Entry event was defined by the spacecraft
reaching an altitude of 400,000 feet, the U or radial position
errors, could only be negative. Consequently, the U errors
are not normally distributed. Since the relationship between
the downrange and radial position errors is quadratic rather
than linear, the correlation coefficient between the two vari-
ates is nearly zero. The expected strong negative correlation
between downrange position and radial velocity errors is present.

The other components of the errors were relatively
loosely correlated. By far the largest component of velocity
error was in the out-of-plane ($\dot{W}$) direction which causes an
azimuth error. No regression analysis was done on the statis-
tics. However, by comparing samples with large out-of-plane
velocity errors at Entry to the errors which were present at
the end of TEI, it appears that there is a strong correlation
between out-of-plane velocity errors at Entry and out-of-plane
velocity errors at the end of TEI. The midcourse corrections
took care of the out-of-plane position error at Entry but could
not take care of the velocity error.

Two other quantities were also computed at Entry.
These were the flight path angle, and the geocentric azimuth
(measured clockwise from North). The means and the standard
deviations of the distributions of these two quantities are
presented in Table 5. In addition, the cumulative distribution
functions for each of the quantities was plotted and is pre-
sented in Figures 2 and 3 respectively. The star curves on
each of the plots are gaussian cumulative distributions with
the same mean and variance as the sample mean and variance of
the plotted distributions.

The distributions of the flight path angle and azimuth errors are seen to be very nearly gaussian. The difference between the sample mean of the flight path angle distribution and the reference trajectory value is slightly larger than the value of the sample standard deviation divided by the square root of the number of samples. This indicates that there is a good likelihood that the true mean of the distribution is not equal to the reference trajectory value. The probable bias of .005 degrees is negligibly small however.

The three sigma variation of flight path angle about the sample mean is .399 degrees so that the 99.73% "width" of the required entry corridor is about .798 degrees. Reference 4 presents curves which relate the allowable flight path angle corridor to lift-to-drag ratio. Comparing .798 degrees to the reference 4 data, one concludes that a lift-to-drag ratio as small as .025 could be tolerated, provided the reference trajectory value is appropriately selected. (The reference 4 ten G limit curve had to be extrapolated to the zero L/D point to arrive at this conclusion. A check of the allowable flight path angle dispersions for small L/D was made using an Entry program developed at Bellcomm and the conclusion was verified.)

The difference between the sample mean of the azimuth errors and the reference trajectory value is slightly larger than the expected standard deviation of the sample mean. This indicates that the azimuth errors are probably biased with respect to the reference value. The probable bias of .025° is negligibly small however. The three sigma variation in the azimuth error of $\pm$ .42 degrees can be easily handled during the Entry phase.

Table 6 presents a summary of the statistics of the ΔV required for each of the midcourse corrections as well as the total ΔV, for the entire transearth leg of the mission.

The first correction was made 95.1% of the time and almost all of those used the SPS engine. The assumption that the first correction would be made at nineteen hours after TEI forces the ΔV required to be considerably larger than it would be if the time of the midcourse were selected on the basis of the magnitude of the required correction. Current mission plans provide for the correction to be made anywhere in a band of time, e.g., anywhere from nine to twenty-five hours after TEI. In this particular case, the TEI errors were so large that many of the corrections would have been made nine or ten hours after injection at considerable savings in SPS fuel.

Similarly, several of the samples fell into the gap between five and seventeen fps for the first midcourse and so were not made. Many of these required substantial second corrections and forced the second midcourse statistics to be rather pessimistic as well. One sample, for example, had a required ΔV for the first midcourse of 15.3 fps. By the time of the second correction, the required ΔV had grown to 113 fps. Under current mission plans, a first correction would have been made using either the RCS system only around ten hours after TEI or the SPS system around twenty hours after TEI.

The required ΔV for the second midcourse was substantially less than for the first correction. A quarter of the corrections requiring the SPS engine were samples in which the first correction requirement fell into the five to seventeen fps gap. About half of the second corrections required from one to five fps and were made with the RCS system only.

The third correction was not required in 25% of the cases. About half of the corrections made required the RCS system only. Most of the cases requiring the SPS system were again samples in which the previous midcourse required ΔV fell between five and seventeen fps. Recall, that for the third correction, the RCS system was to be used for required ΔV's in the five to seventeen fps range. Interestingly, an extremely small percentage (less than 1%) fell into this range.

In general, the SCS ΔV mode performed the corrections surprisingly well considering the error statistics assumed for the system. The total transearth midcourse requirements exceeded 100 fps in 38% of the cases. This, of course, would be unacceptable, but a more flexible method for selecting the time of the correction would improve the midcourse statistics considerably.

Figures 4, 5, and 6 present the cumulative distribution of the total RCS, SPS, and combined ΔV required for the entire transearth leg. The star curves again are normal distributions with the same mean and variance as the plotted distributions.

4.0   CONCLUSIONS

The SCS system when used as the backup guidance system in the SCS ΔV mode results in considerably degraded performance when compared to the primary guidance system. Velocity errors at the end of transearth injection are, in the neighborhood of

fifteen times larger for the SCS system. The resulting errors achieved at Entry are substantially larger than those achieved by the primary system, but they are acceptably small. The flight path angle errors at Entry were .399 degrees (3 sigma) so that the proposed spacecraft lift-to-drag ratio of 0.26 would be adequate in this case. The midcourse fuel requirements for the SCS ΔV mode are larger than for the primary system, but with a reasonable time of midcourse correction selection criteria, it appears that the required fuel would not be excessive.

The SCS ΔV guidance mode combined with MSFN navigation produces slightly larger errors at Entry than does the primary guidance system with the on board optical navigation system.

ACKNOWLEDGEMENTS

The author would like to express his considerable appreciation to Mr. B. G. Niedfeldt and Mr. M. G. Kelly who generated and verified the free fall transition matrices used in the study and to Mr. D. J. Roek who programmed, debugged, and ran the main Monte Carlo Program used in the study. The entire study (excluding this document) was conducted on a crash basis in a period of three weeks. That would have been impossible without the tireless help of these individuals.

D. A. Corey

2012-DAC-vh

Attachments
Tables 1 through 6
Figures 1 through 6

BELLCOMM, INC.

REFERENCES

1. Summary of Apollo Guidance and Navigation Error Analysis, TR-66-310-4, D. A. Corey, T. S. Englar, B. G. Niedfeldt, R. V. Sperry, Bellcomm Inc., July 6, 1966.

2. AS-504A Preliminary Spacecraft Reference Trajectory MSC Internal Note No. 66-FM-70, July 1, 1966 (CONFIDENTIAL)

3. A Study of Methods of Augmenting Cross-Product Steering with Direct Control of Out-of-Plane Position Errors - CSM Transearth Injection, - TM-67-2012-3, D. A. Corey, Bellcomm, Inc., August 28, 1967.

4. Impact of Low Vehicle L/D on Apollo Mission - 1967 Version, Apollo Project Memorandum #1735, R. Morth, MIT/IL, June 6, 1967.

5. From material presented at a Program Managers' Review for NASA held at North American Aviation, Downey, California on January 16, 1967.

6. GG 248 Wide Angle Miniature Integrating Gyro - RED 9964-1, Minneapolis Honeywell, February 12, 1964.

7. Design Specification for Apollo Command Module SCS - Block I A 65-750A3(5) Minneapolis Honeywell, February 1, 1965.

TABLE 1
ERROR SOURCE VALUES

Error Source	1 σ value	New random sample for each maneuver
x Gyro g sensitive drift	3°/hr/g (1)	No
y Gyro g sensitive drift	3°/hr/g (1)	No
z Gyro g sensitive drift	3°/hr/g (1)	No
Initial misalignment about body roll axis	0.5°	Yes
Initial misalignment about body yaw axis	0.5°	Yes
Initial misalignment about body pitch axis	0.5°	Yes
Accelerometer misalignment in yaw plane	0.06°	No
Accelerometer misalignment in pitch plane	0.06°	No
Center of gravity uncertainty in the yaw plane	0.5° (2)	Yes
Center of gravity uncertainty in the pitch plane	0.5° (2)	Yes
x Gyro Constant drift	2.333°/hr (3)	No
y Gyro Constant drift	2.333°/hr (3)	No
z Gyro Constant drift	2.333°/hr (3)	No
Delta V counter uncertainty	.004333 x Delta V (4) for the maneuver or 0.25 fps whichever is greater	Yes
SPS Thrust uncertainty	200 lb.	No
SPS Specific Impulse uncertainty	3.149 Sec.	No
RCS Thrust uncertainty	4 lb.	No
RCS Specific Impulse uncertainty	2.8 Sec.	No
Mass uncertainty (beginning of TEI)	10.244 slugs	---

(1) reference 6 actually states 1.333°/hr/g

(2) reference 5

(3) reference 6

(4) reference 7

TABLE 2

Characteristics of the Reference Trajectory
and Nominal Vehicle

Transearth Flight Time	99 hr 2 min 14.540 sec.
TEI Burn Time	119.603 sec.
TEI ΔV (guided)	2654.3182 fps
$\left| V_{inf} \right|$	2661.7 fps
Eccentricity at TEI	1.2532
Selenographic Inclination of TEI	173.890°
Selenographic Longitude of the ascending Node	25.677°
Geographic Latitude of Entry	-9.413°
Geographic Longitude of Entry	156.829
Altitude of Entry	401853.6 feet
Flight Path Angle at Entry	-6.266°
Geocentric Azimuth at Entry	126.957
Velocity at Entry	36069.5 fps
Geographic Inclination at Entry	37.913°
Geographic Longitude of the Ascending Node	16.937°
Vehicle Weight at TEI Ignition	32959.0 lb.
Vehicle Weight at TEI Cut-off	25362.7 lb.
SPS Engine Thrust	20000 lb.
RCS Total Thrust	400 lb.

TABLE 3

STATISTICS AT THE END OF TRANSEARTH INJECTION

SAMPLE COVARIANCE MATRIX OF ACTUAL DEVIATIONS

	U(feet)	V(feet)	W(feet)	$\dot{U}$(fps)	$\dot{V}$(fps)	$\dot{W}$(fps)	MASS(Slugs)
U	.1636 E8	-.2016 E7	-.1632 E7	.2450 E6	-.1789 E5	-.2349 E5	.1593 E4
V	-.2016 E7	.5634 E7	-.2502 E6	-.3677 E5	.3523 E4	-.7443 E4	-.1350 E5
W	-.1632 E7	-.2502 E6	.1448 E8	-.2427 E5	-.7141 E4	.2147 E6	-.3401 E3
$\dot{U}$	.2450 E6	-.3677 E5	-.2427 E5	.3678 E4	-.2506 E3	-.3441 E3	.3981 E2
$\dot{V}$	-.1789 E5	.3523 E4	-.7141 E4	-.2506 E3	.2383 E3	-.9811 E2	-.1005 E2
$\dot{W}$	-.2349 E5	-.7443 E4	.2147 E6	-.3441 E3	-.9811 E2	.3188 E4	.3757 E1
MASS	.1593 E4	-.1350 E5	-.3401 E3	.3981 E2	-.1005 E2	.3757 E1	.7124 E2

SAMPLE MEANS OF ACTUAL DEVIATIONS

U(feet)	V(feet)	W(feet)	$\dot{U}$(fps)	$\dot{V}$(fps)	$\dot{W}$(fps)	MASS(Slugs)
-.5189 E2	-.1407 E3	.1759 E3	-.6886 E0	-.2255 E1	.2641 E1	-.1035 E0

SAMPLE STANDARD DEVIATIONS OF ACTUAL DEVIATIONS

U(feet)	V(feet)	W(feet)	$\dot{U}$(fps)	$\dot{V}$(fps)	$\dot{W}$(fps)	MASS(Slugs)
.4045 E4	.2374 E4	.3805 E3	.6065 E2	.1544 E2	.5646 E2	.8440 E1

TABLE 4

STATISTICS AT ENTRY

SAMPLE COVARIANCE MATRIX OF ACTUAL DEVIATIONS

	U (feet)	V (feet)	W (feet)	$\dot{U}$ (fps)	$\dot{V}$ (fps)	$\dot{W}$ (fps)	MASS (Slugs)
U	.9689 E5	.2043 E6	-.4683 E5	-.1187 E4	-.3960 E3	.2293 E4	.1245 E3
V	.2043 E6	.5826 E10	.1217 E8	-.5340 E7	-.5870 E6	.5576 E6	-.2456 E5
W	-.4683 E5	.1217 E8	.8616 E7	-.7992 E4	-.1321 E3	-.5803 E4	-.1615 E4
$\dot{U}$	-.1187 E4	-.5340 E7	-.7992 E4	.8353 E4	.1179 E4	-.2368 E4	.5287 E2
$\dot{V}$	-.3960 E3	-.5870 E6	-.1321 E3	.1179 E4	.2329 E3	-.2984 E3	.1071 E2
$\dot{W}$	.2293 E4	.5576 E6	-.5803 E4	-.2368 E4	-.2984 E3	.1776 E5	-.1248 E2
MASS	.1245 E3	-.2456 E5	-.1615 E4	.5287 E2	.1071 E2	-.1248 E2	.8090 E2

SAMPLE MEANS OF ACTUAL DEVIATIONS

	U (feet)	V (feet)	W (feet)	$\dot{U}$ (fps)	$\dot{V}$ (fps)	$\dot{W}$ (fps)	MASS (Slugs)
	-.1374 E3	.2513 E4	.3453 E2	-.8165 E1	-.1269 E1	.1499 E2	-.7625 E1

SAMPLE STANDARD DEVIATIONS OF ACTUAL DEVIATIONS

	U (feet)	V (feet)	W (feet)	$\dot{U}$ (fps)	$\dot{V}$ (fps)	$\dot{W}$ (fps)	MASS (Slugs)
	.3113 E3	.7633 E5	.2935 E4	.9139 E2	.1526 E2	.1333 E3	.8994 E1

TABLE 5

SUMMARY OF ENTRY ERRORS

Error	Sample Mean	Sample Standard Deviation
Flight Path Angle	-6.2724 deg.	.13298 deg.
Azimuth	126.932 deg.	.21609 deg.

TABLE 6

MIDCOURSE ΔV REQUIRED

	MEAN (fps)	STANDARD DEVIATION (fps)	PERCENT MADE
MIDCOURSE 1			
RCS	4.7536	1.0805	95.1
SPS	61.4247	37.3898	94.9
TOTAL	66.1784	37.8083	95.1
MIDCOURSE 2			
RCS	2.0154	2.1451	52.1
SPS	8.3368	22.5766	22.5
TOTAL	10.3522	23.7521	52.1
MIDCOURSE 3			
RCS	3.1071	2.6195	74.6
SPS	16.3968	21.2528	45.2
TOTAL	19.5039	22.8196	74.6
TOTAL TRANSEARTH			
RCS	9.8761	1.9741	73.9
SPS	86.1584	46.3497	54.2
TOTAL	96.0345	47.2634	73.9
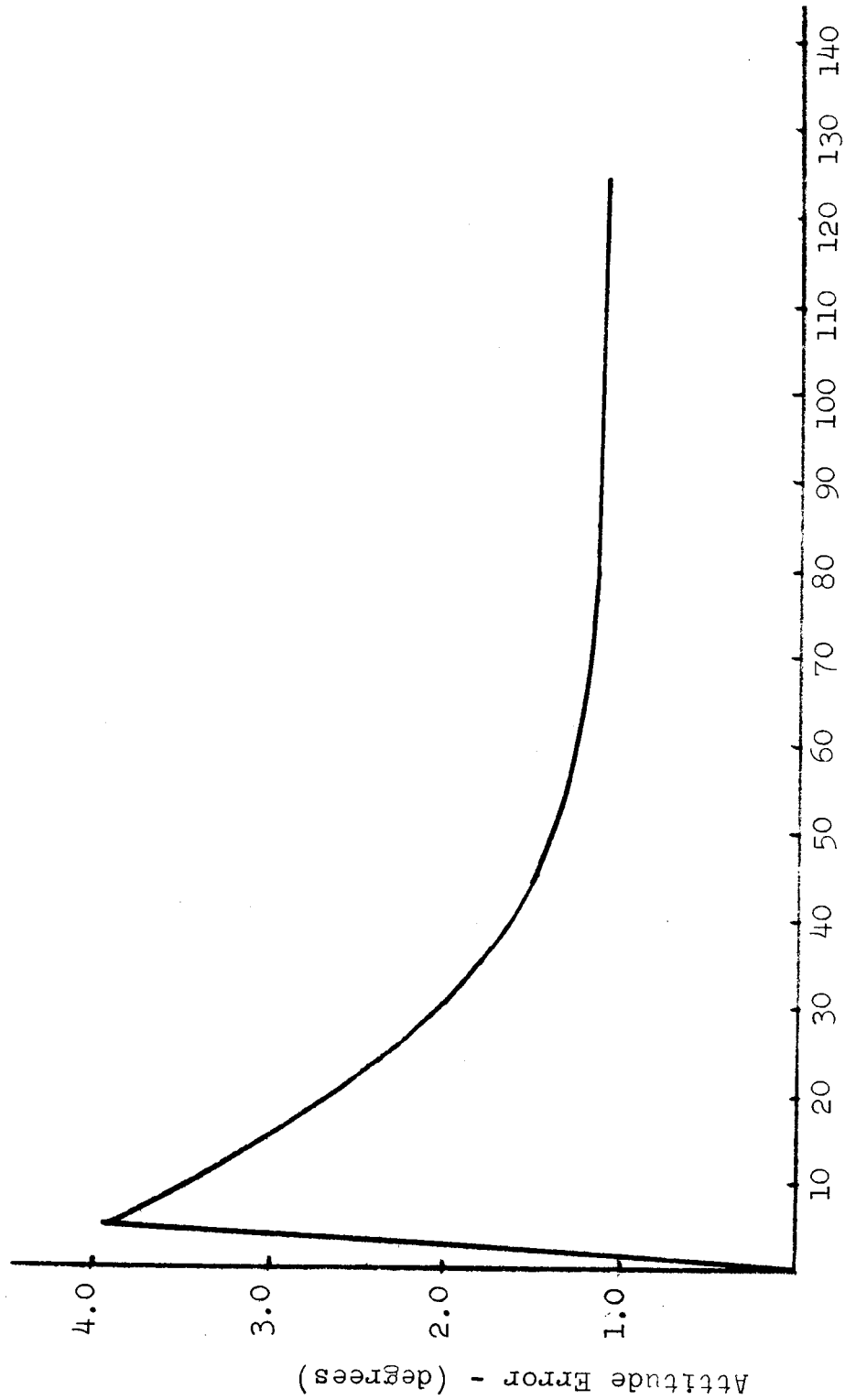
Figure 1   Pitch and Yaw Attitude Error Due to 1.5° (3σ) Center
of Gravity Uncertainty

FIGURE 2

CUMULATIVE DISTRIBUTION   PATH ANGLE

The solid line indicates the curve
obtained from the sample data. The
curve formed by the star points
represents a normal distribution
with mean and variance equal to the
sample mean and variance.

FIGURE 3

The solid line indicates the curve obtained from the sample data. The curve formed by the star points represents a normal distribution with mean and variance equal to the sample mean and variance.

FIGURE 4

CUMULATIVE DISTRIBUTION   DV-ACT MAG.

MSC SPECIAL DATA CASE (504 PRT) *SCS DLV*

ΔV (FPS)

ACTUAL   RCS TRANS-EARTH

The solid line indicates the curve obtained from the sample data. The curve formed by the star points represents a normal distribution with mean and variance equal to the sample mean and variance.

FIGURE 5

CUMULATIVE DISTRIBUTION   DV-ACT MAG.

MSC SPECIAL DATA CASE (504 PRT) *SCS DLV*

ACTUAL   SPS TRANS-EARTH

V (FPS)

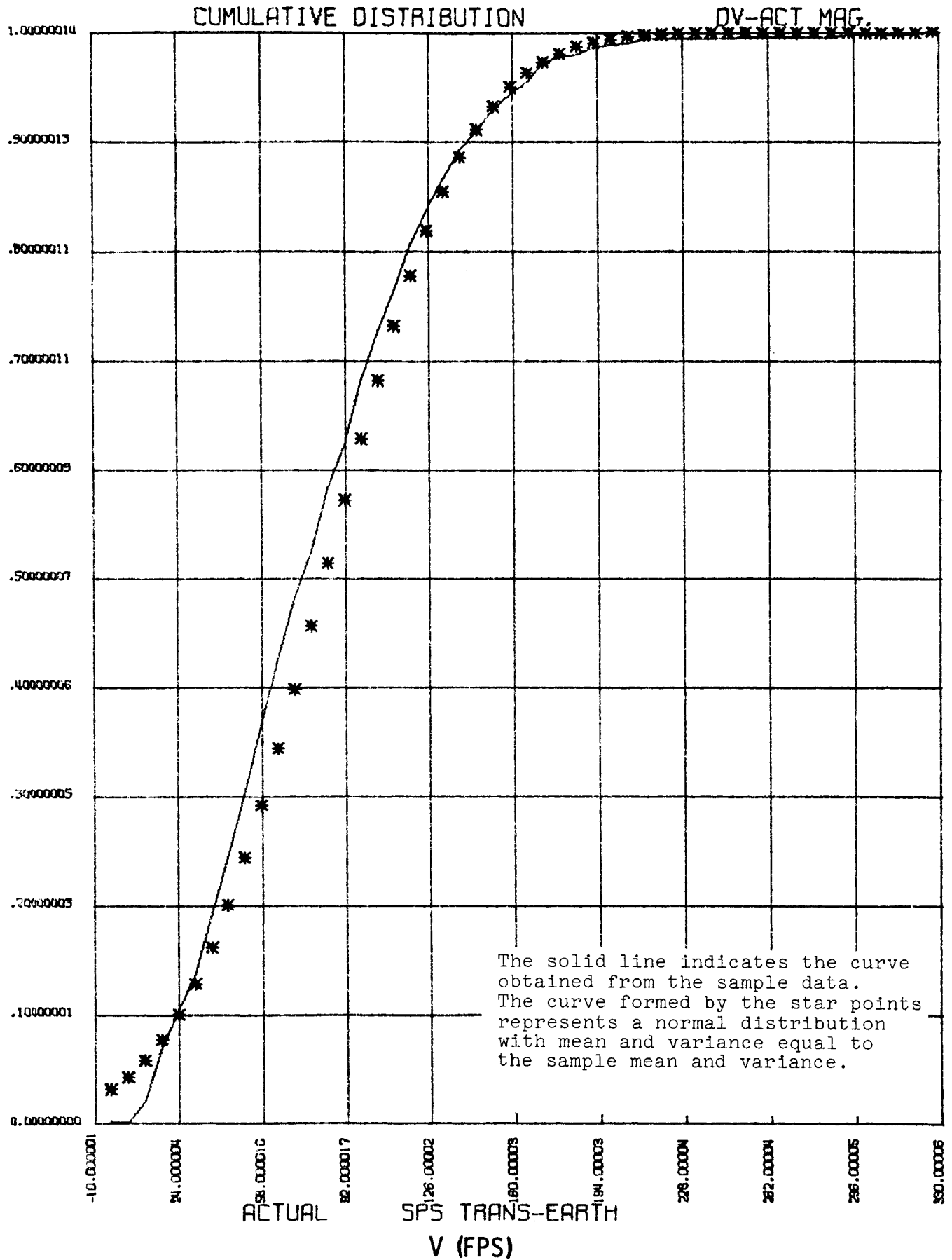The solid line indicates the curve
obtained from the sample data.
The curve formed by the star points
represents a normal distribution
with mean and variance equal to
the sample mean and variance.

FIGURE 6

The solid line indicates the curve obtained from the sample data. The curve formed by the star points represents a normal distribution with mean and variance equal to the sample mean and variance.